2) Simonetti J, Bulkow L, McMahon BJ, et al : Clearance of hepatitis B surface antigen and risk of hepatocellular carcinoma in a cohort chronically infected with hepatitis B virus. Hepatology　2010 ; 51 : 1531-1537

3) Lau GK, Piratvisuth T, Luo KX, et al : Peginterferon Alfa-2a, lamivudine, and the combination for HBeAg-positive chronic hepatitis B. N Engl J Med 2005 ; 352 : 2682-2695

4) Buster EH, Flink HJ, Cakaloglu Y, et al : Sustained HBeAg and HBsAg loss after long-term follow-up of HBeAg-positive patients treated with peginterferon alpha-2b. Gastroenterology　2008 ; 135 : 459-467

5) Marcellin P, Bonino F, Lau GK, et al : Sustained response of hepatitis B e antigen-negative patients 3 years after treatment with peginterferon alpha-2a. Gastroenterology　2009 ; 136 : 2169-2179, e1-e4

6) Marcellin P, Lau GK, Bonino F, et al : Peginterferon alfa-2a alone, lamivudine alone, and the two in combination in patients with HBeAg-negative chronic hepatitis B. N Engl J Med　2004 ; 351 : 1206-1217

7) Lampertico P, Vigano M, Colombo M : Treatment of HBeAg-negative chronic hepatitis B with pegylated interferon. Liver Int　2011 ; 31(Suppl 1) : 90-94

8) Lai CL, Shouval D, Lok AS, et al : Entecavir versus lamivudine for patients with HBeAg-negative chronic hepatitis B. N Engl J Med　2006 ; 354 : 1011-1020

9) Lampertico P, Viganò M, Di Costanzo GG, et al : Randomised study comparing 48 and 96 weeks peginterferon α-2a therapy in genotype D HBeAg-negative chronic hepatitis B. Gut　2013 ; 62 : 290-298

10) Hosaka T, Suzuki F, Kobayashi M, et al : Clearance of hepatitis B surface antigen during long-term nucleot(s)ide analog treatment in chronic hepatitis B : results from a nine-year longitudinal study. J Gastroenterol　2013 ; 48 : 930-941

11) Marcellin P, Gane EJ, Tsai N, et al : Seven years of treatment with tenofovir DF for chronic hepatitis B virus infection is safe and well tolerated and associated with sustained virological, biochemical and serological responses with no detectable resistance. Hepatology　2013 ; 58 : A649

12) Kim GA, Lim YS, An J, et al : HBsAg seroclearance after nucleoside analogue therapy in patients with chronic hepatitis B : clinical outcomes and durability. Gut　2013 Oct 25. (Epub ahead of print)

13) Papatheodoridis G, Goulis J, Manolakopoulos S, et al : Changes of HBsAg and interferon-inducible protein 10 serum levels in naive HBeAg-negative chronic hepatitis B patients under 4-year entecavir therapy. J Hepatol　2014 ; 60 : 62-68

14) Ouzan D, Pénaranda G, Joly H, et al : Add-on peginterferon leads to loss of HBsAg in patients with HBeAg-negative chronic hepatitis and HBV DNA fully suppressed by long-term nucleotide analogs. J Clin Virol　2013 ; 58 : 713-717

15) Boglione L, D'Avolio A, Cariti G, et al : Sequential therapy with entecavir and PEG-INF in patients affected by chronic hepatitis B and high levels of HBV-DNA with non-D genotypes. J Viral Hepatol 2013 ; 20(4) : e11-e19

16) Sonneveld MJ, Rijckborst V, Boucher CA, et al : Prediction of sustained response to peginterferon alfa-2b for hepatitis B e antigen-positive chronic hepatitis B using on-treatment hepatitis B surface antigen decline. Hepatology　2010 ; 52 : 1251-1257

17) Ma H, Yang RF, Wei L : Quantitative serum HBsAg and HBeAg are strong predictors of sustained HBeAg seroconversion to pegylated interferon alfa-2b in HBeAg-positive patients. J Gastroenterol Hepatol　2010 ; 25 : 1498-1506

18) Piratvisuth T, Lau G, Marcellin P, et al : On-treatment decline in serum HBsAg levels predicts sustained immune control and HBsAg clearance 6 month posttreatment in HBsAg-positive hepatitis B virus-infected patients treated with peginterferon alfa-2a [40kD] (PEGASYS). Hepatol Int　2010 ; 4 : 152

19) Chan HL, Wong VW, Chim AM, et al : Serum HBsAg quantification to predict response to peginterferon therapy of e antigen positive chronic hepatitis B. Aliment Pharmacol Ther　2010 ; 32 : 1323-1331

20) Moucari R, Mackiewicz V, Lada O, et al : Early serum HBsAg drop : a strong predictor of sustained virological response to pegylated interferon alfa-2a in HBeAg-negative patients. Hepatology　2009 ; 49 : 1151-1157

21) Brunetto MR, Moriconi F, Bonino F, et al : Hepatitis B virus surface antigen levels : a guide to sustained response to peginterferon alfa-2a in HBeAg-negative chronic hepatitis B. Hepatology　2009 ; 49 : 1141-1150

22) Palumbo GA, Belloni L, Valente S, et al : Targeting the cccDNA by epigenetic drugs inhibitors HBV transcription and replication. Hepatology　2013 ; 58 : 650A

肝疾患 Review 2014-2015

第4章　細胞株の凍結保存、溶解、生存率検査の禁止事項とノウハウ

第2節　霊長類 ES／iPS 細胞の凍結保存・輸送・解凍

今松　伸介　(株)リンフォテック

安成　皓　東京工業大学大学院　生命理工学研究科

馬場　憲三　日本ジェネティクス(株)

岡崎　宏吾　(株)リンフォテック

田川　陽一　東京工業大学大学院　生命理工学研究科　教授　博士(理学)

第 2 節　霊長類 ES/iPS 細胞の凍結保存・輸送・解凍

はじめに

培養細胞を取り扱う研究において，細胞の凍結保存は必須の技術である。1949 年にグリセロールが凍結保存されたウシ精子を保護する効果をもつ[1] ことが発見されて以来，様々な凍結保護物質が見出され，細胞の凍結保存が可能になったことで細胞生物学の実験結果の再現性が確認できるようになっただけでなく，生殖・細胞移入医療や家畜産業等も大きく発展した。細胞の凍結保存の手法は，一般に緩慢凍結法と急速凍結法（ガラス化法）に大別される。

緩慢凍結法は，グリセロールやジメチルスルホキシド（DMSO）を凍結保護物質とし，1 分に 1℃程度に温度を下げて徐々に凍結する方法であり，多様な細胞を凍結保存できることが報告されている[2-5]。緩慢に冷却することで細胞内の水分子が凍結保護剤と置換し脱水され，細胞内及び細胞周辺部の氷結晶の成長が抑えられ，細胞膜・細胞内構造の損傷や，タンパク質の変性・切断を防ぐ[6]。プログラムフリーザーで厳密に温度調節して凍結することが必要とされていたが，胚の凍結保存を除き一般的な細胞では，発砲スチロールの箱や市販の細胞凍結ボックスを用いて緩慢に凍結する方法が研究室や細胞バンク等で主流である。また，解凍時は 37℃のウォーターバスで急速に融解する。このような手法を簡易緩慢凍結法と呼ぶ場合もある。操作が容易であり，多くの細胞種や細胞株でこの緩慢凍結法が用いられている。

これに対し，1937 年に提唱されたガラス化法は，細胞内外の水を液体窒素で急速に冷却し，ガラス化状態で凍結保存する手法である。ガラス化とは，分子が規則正しい結晶構造をとらないで固体と同程度の固さになる現象を指す。理想的な実用技術になると考えられてきたが，その成功例は長く得られなかった。

しかし，1985 年に高濃度の凍結保護剤を用いることにより，マウス初期胚の凍結保存に成功した[7] ことで哺乳動物胚の新たな凍結保存法としての可能性が示された。この成功を機に，様々な哺乳動物胚の凍結保存が可能になった[8-10]ことから，ガラス化法は胚バンクをはじめ多くの機関で用いられている。

1.　霊長類 ES/iPS 細胞の性質と凍結保存の現状

マウス胚性幹（Embryonic Stem ; ES）細胞は 1981 年に樹立[11] されて以来の歴史の中で，樹立・培養・凍結の最適条件が見出されてきた。マウス ES 細胞は遺伝子導入後のスクリーニング待ちの間，プレート上でコロニーのまま保存[12] することも可能なくらい，他の一般的な細胞株よりも凍結抵抗性に優れているようにも思える。しかし，霊長類 ES 細胞はサルで 1995 年[13]，ヒトでは 1998 年[14] に樹立されたこともあり，これらの細胞取扱い技術は開発途上である。マウス ES 細胞の場合はキメラマウスを作製し，そのマウスのキメラ率や生殖系列伝達を確認できることで ES 細胞としての性質の標準化が明確である。しかし，霊長類 ES 細胞の場合はそのような実験が不可能なために標準化が曖昧になっていることが，霊長類 ES 細胞の培養や凍結の最適条件が決まらない理由でもある。またこのような状況の中で，2007 年にヒト ES 細胞とほとんど等価であるとされるヒト人工万能性幹（induced Pluripotent Stem ; iPS）細胞が体細胞から人工的に作出され[15]，ヒト ES 細胞と同様な条件で取り扱われている。

マウスとヒト（霊長類）で同じように ES/iPS 細胞と呼ばれているが，それらが有する細胞生物学的な性質は異なる[16]。その一つとして，マウス ES/iPS 細胞は未分化維持のためにはコロニーを酵素処理により単一細胞にして継代を行うが，霊長類 ES/iPS 細胞を単一細胞に解離させてしまうと細胞死（アポトーシス）が誘導[17,18] されるために，コロニーを 10 ～ 50 程度にして細胞間接着を保ったまま行わなければならない。継代時だけでなく，凍結・解凍する際も同様である。もう一つは，緩慢凍結法における解凍後の回復率の違いがあげられる。マウス ES/iPS 細胞は，操作の簡便性や解凍後の回復率の良さなどを考慮して市販の凍結保存液を使用する研究者も多いが，一般の細胞株と同様に 10% DMSO を含有した培地／ウシ胎仔血清を用い緩慢凍結法により凍結保存することができる。一方，霊長類 ES/iPS 細胞の細胞塊を 10% DMSO 含有培地で緩慢凍結法により凍結保存すると，解凍後の回復率が著しく低い[19]。細胞内に形成される氷結晶が細胞構造に損傷を与えている可能性がある[6] が，胚のような細胞集団を凍結するときもこの方

法では凍結できないことを考えると細胞塊の状態は緩慢凍結法には向いていないのかも知れない。そのため，新規の凍結保存液の開発が望まれている。

　細胞質の容積が他の細胞に比べて大きい，または単一細胞ではなく複数の細胞（割球）で構成されている初期胚はガラス化法で凍結保存する。細胞塊の状態で凍結保存をするヒト ES 細胞の凍結保存もガラス化法が用いられるようになった[20]。これは，ガラス化保存液中に細胞塊を懸濁し，哺乳類の初期胚などを凍結保存する際に用いるストロー内に移した後に液体窒素に直接浸漬して急速にガラス化状態にする方法である。また，将来的な医療への応用を考慮し，ガラス化保存液に含まれているウシ胎仔血清をヒトアルブミンに置き換えることで異種成分を排除することも可能となった[21]。しかし，これらのストローを用いるガラス化法は，凍結・解凍の操作が煩雑であり，またごく少量の細胞しか凍結保存できないという欠点があった。その後，ストローの代わりに凍結チューブを用いても凍結保存が可能であることが示され，ガラス化保存液の組成を最適化することにより，緩慢凍結法よりも劇的に回復率が向上した[19]。この凍結法を簡易ガラス化法と呼ぶ場合もある。この方法により，従来のガラス化法よりも操作性が向上し，さらにより多くの細胞を凍結保存できるようになった。日本国内では霊長類 ES/iPS 細胞の凍結保存には主にこの方法が用いられている。なお，米国・カナダでは，回復効率が悪くても，一般的な 10% DMSO 含有培地で操作が簡便な緩慢凍結法により凍結保存している研究者が多い。

2.　ドライアイス輸送を考慮した霊長類 ES/iPS 細胞用凍結保存液の開発

　我国内では霊長類 ES/iPS 細胞の凍結保存は，ガラス化法が主流である。しかしながらガラス化保存液はその高い浸透圧のため，細胞をガラス化保存液に懸濁してから液体窒素に浸漬するまで 15 〜 30 秒程度という短時間に行わなければ解凍後の回復率が極端に低くなってしまう[19]。そのため，操作には熟練を必要とする。また，ガラス化保存液は − 130℃より高い温度で保存するとガラス化した水が脱ガラス化し，細胞内外で再結晶することによって細胞膜・細胞内構造に損傷を与えてしまうため，ガラス化細胞はドライアイスで輸送することができない。そのため，液体窒素中で輸送する必要があり，特別な液体窒素輸送箱が必要となり輸送費用もかさむ（図 1）。
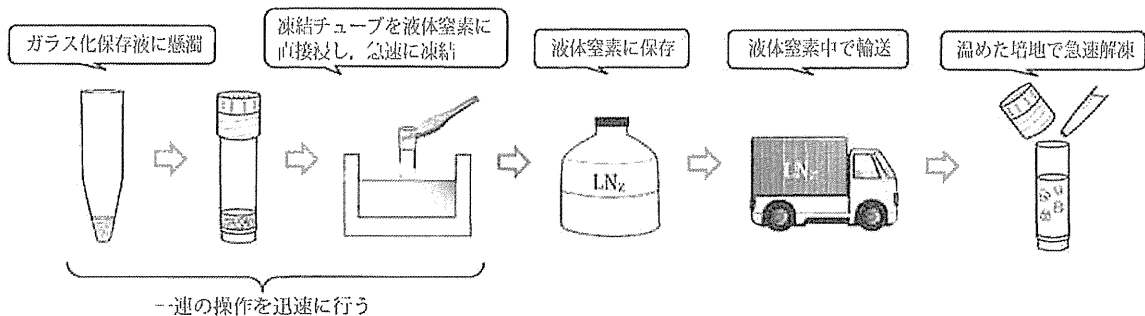
A) 緩慢凍結法
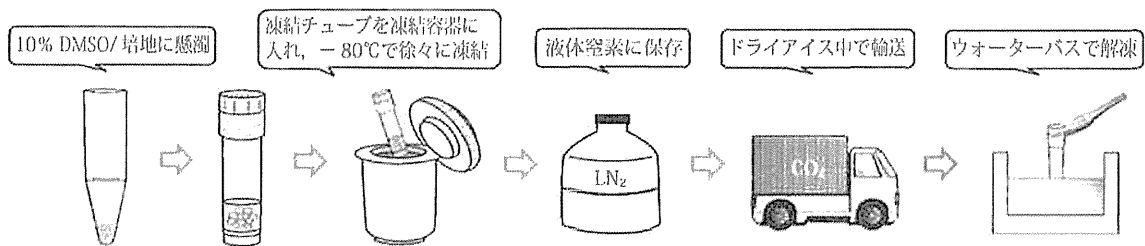
B) ガラス化法

図 1　細胞の凍結 − 保存 − 輸送 − 解凍の流れ

　そこで筆者らは，上記の問題を克服するため，凍結保護剤であるDMSOとヒト血清アルブミンの2つの成分に着目し，霊長類ES/iPS細胞の緩慢法凍結保存液を開発した（製品名：バンバンカー ®hRM　以下開発品とする）。そして，開発品によるサル（コモンマーモセット）ES細胞の凍結・解凍後の回復率，及びドライアイス輸送における安定性を検討した。

　セミコンフルエント状態のサルES細胞コロニーを分割して培養容器から剥離し，開発品を用いて緩慢凍結法で凍結した。コントロールとして，一つに既存のガラス化保存液でガラス化法，もう一つに10% DMSOを含む霊長類ES/iPS細胞用培地で緩慢凍結法によりそれぞれ凍結した。解凍後，培養4日目にアルカリホスファターゼ染色を行い，未分化状態の生着コロニー数を比較した（図2）。その結果，開発品は，既存のガラス化保存液と比較し約2倍，10% DMSOを含む培地と比較し，約4倍生着コロニー数が多いことが示された（図3）。

(a)　　　　　　　　　　　(b)

（a）コロニーの顕微鏡写真　　　（b）アルカリホスファターゼ染色

図2 解凍後のサルES細胞

＊P＜0.05
＊＊P＜0.01
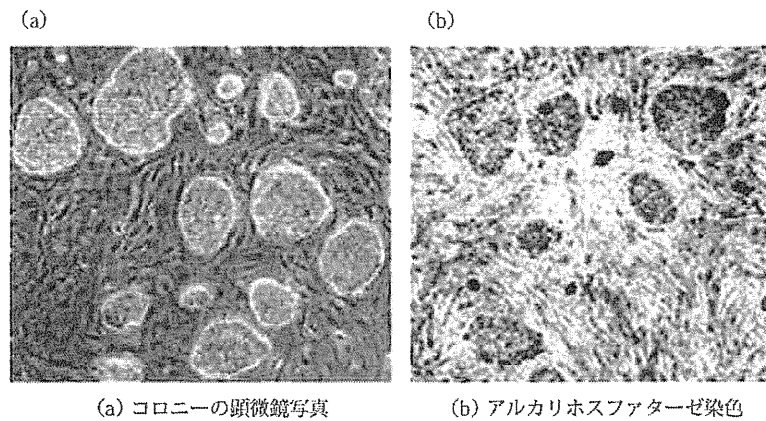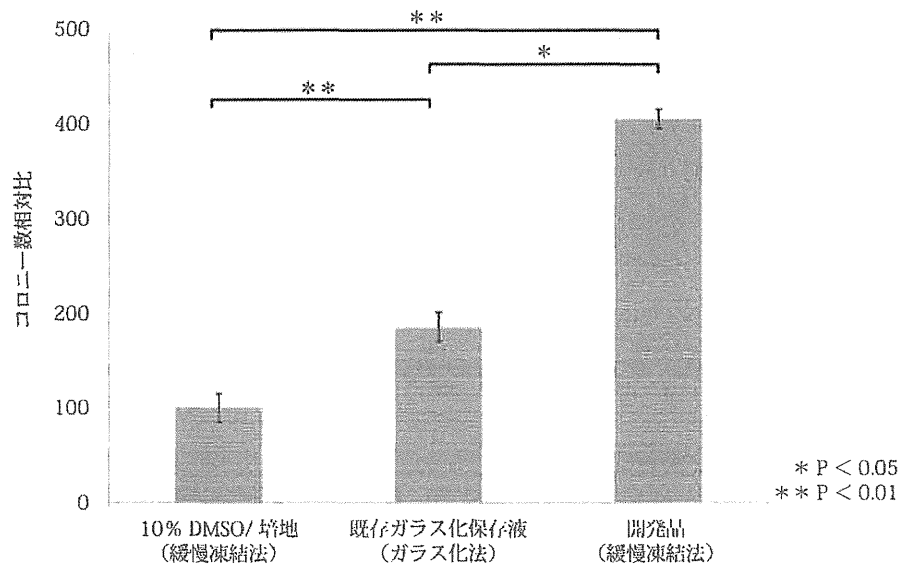
10% DMSO/ 培地で凍結・解凍して得られた未分化状態の生着コロニー数を100とした場合の生着コロニー数相対比を表している。

図3　各凍結保存液の解凍後生着コロニー数相対比

　さらに，開発品で凍結した細胞のドライアイス中での安定性を検討した。開発品で凍結した細胞を液体窒素に保存した後，ドライアイス中に移して24時間保存した。解凍後，培養4日目にアルカリホスファターゼ染色を行い未分化状態の生着コロニー数を測定した。その結果，ドライアイス保存後でも未分化状態を維持した生着コロニーが十分得られ

ることが確認できた。一方で、ガラス化法で凍結した細胞で同様の試験を行った場合は生着コロニーはほとんど確認できず、ガラス化法で凍結保存したサル ES 細胞はドライアイス輸送ができないことを確認した。以上の結果より、開発品を用いることにより、操作が容易な緩慢凍結法でサル ES 細胞の高効率な凍結保存が可能であり、凍結細胞をドライアイスで輸送できることが示された。

3. ROCK 阻害剤を用いた霊長類 ES/iPS 細胞の凍結保存

前述の通り、霊長類 ES/iPS 細胞を単一細胞にしてしまうとアポトーシスが誘導されるため、細胞間接着を保ったままあらゆる操作を行わなければならない。そのため、熟練された技術が必要であり、研究発展の大きな障害となっていた。しかし近年、Rho 結合リン酸化酵素（Rho-associated protein kinase：ROCK）に対する特異的阻害剤である Y-27632 や HA-1077 が単一細胞状態のヒト ES 細胞の生存を飛躍的に向上させることが示され[18]、凍結保存にも応用されている[22,23]。筆者らも緩慢凍結法においては他の細胞株と同じように単一細胞の方がより効果的に凍結保存できるのではないかと考え、ヒト iPS 細胞を凍結前または解凍・播種後に Y-27632 を含む培地で培養するという条件の下、開発品を用いてヒト iPS 細胞を単一細胞状態で凍結し、解凍後の回復率を検討した。

セミコンフルエント状態のヒト iPS 細胞を凍結する 1 時間前に Y-27632 を添加した培地で培養し、トリプシンにより培養容器から剥離し単一細胞にした後、開発品を用いて緩慢凍結法で凍結保存した。解凍後、Y-27632 を添加した培地で 16 時間培養した（表 1）。その後は通常の培地で培養し、培養 8 日目にアルカリホスファターゼ染色を行い、未分化状態のコロニー数を測定した。

その結果、Y-27632 未添加の条件と比較し、細胞を凍結する前に Y-27632 を添加した培地で培養することで約 4 倍、細胞を解凍した後に Y-27632 を添加した培地で培養することで約 5 倍コロニー数が多いことが示された。さらに凍結前・解凍後どちらの培地にも添加すると約 15 倍と劇的にコロニー数が増加した（図 4）。以上より Y-27632 と開発品を組み合わせることにより凍結・解凍時の操作が簡便になりかつ高効率にヒト iPS 細胞を凍結保存できることが示された。

表 1　Y -27632 の培地への添加条件

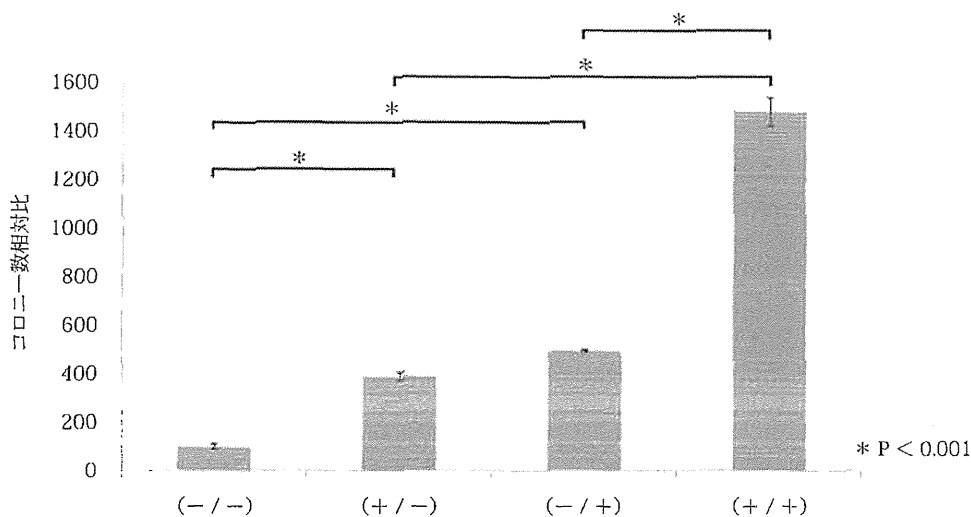| 凍結前	解凍後	
-	-	（-／-）
+	-	（+／-）
-	+	（-／+）
+	+	（+／+）

図 4　凍結前・解凍後における Y-27632 の効果

4. 今後に向けて

　霊長類 ES/iPS 細胞の凍結保存は研究者を満足させるようなレベルには達しておらず，開発途上の技術であるといっても過言ではない。特に解凍後の回復率はまだ低く，改善の余地が多く残されている。今後の基礎研究や再生医療の発展のためには，耐凍メカニズムを詳細に解析し，より回復率が高い凍結保存液の開発が必須であると考えている。

文　　　献

1) Polge, C. et al. : Nature 164 : 666-666 (1949)

2) Polge, C and lovelock, J. E. : Vet. Rec. 64 : 396-397 (1952)

3) Ashwood-Smith, M. J. and Loutit, J. F. : Blood 23 : 494-501 (1964)

4) Pegg, D. E. : J. appl. Phisiol. 19 : 123-126 (1964)

5) Whittingham, D. G et al. : Science 187 : 411-414 (1972)

6) Dobrinsky, J. R. : Theriogenology 45 : 17-26 (1996)

7) Rail, W.F. and Fahy, G. M. : Nature 313 : 573-575 (1985)

8) Vajta, G. et al. : Cryo-Letters 18 : 191-195 (1997)

9) Vajta, G. et al. : Mol. Reprod. Dev. 51 : 53-58 (1998)

10) Vajta, G. et al. : Acta Vet. Scand. 38 : 349-352 (1997)

11) Evans, M. J. and Kaufman, M. H. : Nature 292 : 154-156 (1981)

12) 田川陽一ほか：細胞工学 14 : 946-955 (1995)

13) Thomson, J. A. et al. : Proc. Natl. Acad. Sci. U.S.A 92 : 7844-7848 (1995)

14) Thomson, J .A. et al. : Science 282 : 1145-1147 (1998)

15) Takahashi, K. et al. : Cell 131 : 861-872 (2007)

16) Yu, J. and Thomson, J. A. : Genes Dev. 22 : 1987-1997 (2008)

17) Suemori, H. et al. : Dev. Dyn. 222 : 273-279 (2001)

18) Watanabe, K. et al. : Nat. Biotechnol. 25 : 681-686 (2007)

19) Fujioka, IT. et al. : Int.J. Dev. Biol. 48 : 1149-1154 (2004)

20) Reubinoff, B. E. et al. : Hum. Reprod. 16 (10) : 2187-2194 (2001)

21) Richards, M. et al. : Stem Cells 22 : 779-789 (2004)

22) Li, X. et al. : Hum. Reprod. 24 : 580-589 (2009)

23) Baharvand, H. et al. : Nat. Protoc. 5 (3) : 588-594 (2010)
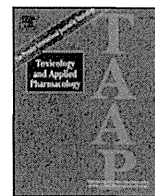
Mitochondrial iron accumulation exacerbates hepatic toxicity caused by hepatitis C virus core protein

Shuichi Sekine [a], Konomi Ito [a], Haruna Watanabe [a], Takafumi Nakano [a], Kyoji Moriya [b], Yoshizumi Shintani [b], Hajime Fujie [b], Takeya Tsutsumi [b], Hideyuki Miyoshi [b], Hidetake Fujinaga [b], Seiko Shinzawa [b], Kazuhiko Koike [b], Toshiharu Horie [a,*]

[a] Laboratory of Biopharmaceutics, Graduate School of Pharmaceutical Sciences, Chiba University, 1-8-1 Inohana, Chuo-ku, Chiba 260-8675, Japan
[b] Department of Internal Medicine, Graduate School of Medicine, The University of Tokyo, 7-3-1 Hongo, Bunkyo-ku, Tokyo 113-8655, Japan

ABSTRACT

Patients with long-lasting hepatitis C virus (HCV) infection are at major risk of hepatocellular carcinoma (HCC). Iron accumulation in the livers of these patients is thought to exacerbate conditions of oxidative stress. Transgenic mice that express the HCV core protein develop HCC after the steatosis stage and produce an excess of hepatic reactive oxygen species (ROS). The overproduction of ROS in the liver is the net result of HCV core protein-induced dysfunction of the mitochondrial respiratory chain. This study examined the impact of ferric nitrilacetic acid (Fe-NTA)-mediated iron overload on mitochondrial damage and ROS production in HCV core protein-expressing HepG2 (human HCC) cells (Hep39b cells). A decrease in mitochondrial membrane potential and ROS production were observed following Fe-NTA treatment. After continuous exposure to Fe-NTA for six days, cell toxicity was observed in Hep39b cells, but not in mock (vector-transfected) HepG2 cells. Moreover, mitochondrial iron (^{59}Fe) uptake was increased in the livers of HCV core protein-expressing transgenic mice. This increase in mitochondrial iron uptake was inhibited by Ru360, a mitochondrial Ca^{2+} uniporter inhibitor. Furthermore, the Fe-NTA-induced augmentation of mitochondrial dysfunction, ROS production, and cell toxicity were also inhibited by Ru360 in Hep39b cells. Taken together, these results indicate that Ca^{2+} uniporter-mediated mitochondrial accumulation of iron exacerbates hepatocyte toxicity caused by the HCV core protein.

© 2014 Elsevier Inc. All rights reserved.

Introduction

Hepatitis C virus (HCV) infection is a major cause of chronic liver disease. About 120–200 million people are infected with HCV, increasing their risk of developing chronic hepatitis, cirrhosis, and eventually hepatocellular carcinoma (HCC) (Ikeda et al., 1998; Nishioka et al., 1991). The HCV genome is approximately 9.6 kb in size and encodes a polyprotein of ~3000 amino acids. The large HCV polyprotein is cleaved by host and viral proteases to generate at least ten smaller proteins, including four structural proteins (one core protein, two envelope proteins, and the E1, E2, and p7 ion channels) (Bukh et al., 1995) and six

non-structural proteins (NH2-NS2, NS3, NS4A, NS4B, NS5A, and NS5B-COOH) (Bartenschlager and Lohmann, 2000). These proteins participate in viral replication and also influence cellular functions of the host.

Oxidative stress is commonly observed following HCV infection and is caused by increased levels of cellular reactive oxygen species (ROS) or by changes in cellular antioxidant capacities (Choi and Ou, 2006; Oberley, 2002; Otani et al., 2005). In particular, HCV core protein is known to be closely associated with the mitochondria and causes the increase in host ROS production, lipid peroxidation (Lau et al., 1998; Moriya et al., 2001; Okuda et al., 2002) and mitochondrial Ca^{2+} uptake. HCV core protein also reduces GSH and NADPH concentrations and mitochondrial complex I activities. These undertakings ultimately disrupt mitochondrial membrane permeability and trigger mitochondrial dysfunction (Wang et al., 2010; Wang and Weinman, 2006). As mitochondrial function is the master regulator of cellular energy and apoptotic cell death, mitochondrial injury can culminate in metabolic deficits and steatohepatitis, further exacerbating cell injury and dysfunction.

Due to the relationship between chronic HCV infection and the development of HCC, numerous studies have attempted to identify the HCV proteins that are responsible for hepatocarcinogenesis. These studies indicate that the HCV core protein can promote the immortalization of primary human hepatocytes (Ray et al., 2000), whereas the non-

structural proteins NS3 and NS4B can transform NIH 3T3 cells, either individually or in combination with Ha-ras (Park et al., 2000). Iron overload in the liver, which is associated with the genetic disorder hereditary hemochromatosis, has been thought to increase the risk of HCC by about 200-fold (Bonkovsky et al., 1997; Kowdley, 2004). For example, the livers of patients afflicted with HCV are characterized by the elevated expression of transferrin receptor 1 and hepcidin, both of which stimulate iron uptake into hepatocytes (Bonkovsky et al., 1997; Hayashi et al., 1994). In contrast, iron depletion (in the form of dietary iron restriction and/or phlebotomy) can improve hepatic inflammation and lower serum aminotransferase activity in HCV patients (Hayashi et al., 1994). Thus, a major precipitating factor for the pathogenesis of HCV-related liver disease has been attributed to the augmentation of oxidative stress following iron accumulation. However, no underlying cellular mechanism has yet been elucidated.

This study investigated the effect of iron exposure on mitochondrial dysfunction, ROS production and cell toxicity in human hepatoma cells stably expressing the HCV core protein (Hep39b cells). The underlying mechanism responsible for mitochondrial iron accumulation in Hep39b cells and in the livers of HCV core protein-expressing transgenic mice was also examined.

Materials and methods

Chemicals and reagents. Ferric nitrate nonahydrate, nitrilotriacetic acid (NTA), 5,5′,6,6′-tetrachrolo-1,1′,3,3′-tetraethylbenzimidazolycarbocyanine iodide (JC-1), carbonyl cyanide-m-chlorophenyl hydrazine (CCCP) and G418 disulfate were from Sigma Aldrich (St. Louis, MO). MitoTracker® Red was from Invitrogen (Carlsbad, CA). $^{59}FeSO_4$ was from Perkin-Elmer (Waltham, MA). Ru360 was from Merck Millipore Japan (Tokyo, Japan). MTT [3-(4,5-dimethylthiazol-2-yl)-2,5-diphenyltetrazolium bromide] was from Wako Pure Chemical Industries, Ltd. (Osaka, Japan). Hydroxyphenyl fluorescein (HPF) was from Sekisui Medical Co., Ltd. (Tokyo, Japan). Adenine nucleotide translocator (ANT) goat polyclonal IgG, CCDC109A goat polyclonal IgG and horseradish peroxidase (HRP)-conjugated anti-goat IgG were from Santa Cruz Biotechnology, Inc. (Santa Cruz, CA). All chemicals and solvents were of analytical grade.

Preparation of Fe-NTA. The Fe-NTA complex was prepared as described by Awai et al. (1979). Briefly, ferric nitrate was dissolved in 1 N HCl to form a 50 mM solution, and NTA was dissolved in 1 N NaOH to form a 150 mM solution. Equal volumes of the two solutions were mixed just before the experiment, and the pH was adjusted to 7.4 with $NaHCO_3$.

Assessment of cytotoxicity. Cytotoxicity was assessed by the MTT assay. Briefly, Hep39b and Hepswx cells were seeded into 96 well culture plates at a density of 8.4×10^3 cells/well and were exposed to various concentrations of Fe-NTA the following day, the medium was replaced with fresh medium containing the same component every 24 h. In some conditions, cells were treated with 20 μM Ru360, a mitochondrial Ca^{2+} uniporter inhibitor, for 1 h prior to Fe-NTA exposure. After six days, the cell culture medium was replaced by 50 μl MTT solution (5 mg/ml MTT in phenol red-free Dulbecco's Modified Eagle's Medium (DMEM)), and the cells were incubated for 2 h at 37 °C. To dissolve the reduced MTT crystals, 200 μl isopropanol was added. The absorbance of the dye was measured at a wavelength of 570 nm, and the turbidity of the cells (background absorbance) was measured at a reference wavelength of 630 nm. The absorbance of the controls (Hepswx and Hep39b) was set at 100%, and cytotoxicity was calculated as the absorbance of the experimental sample relative to that of the control.

Assessment of ROS production. ROS production was first assessed by chemiluminescence (CL) analysis. Briefly, cells were seeded into 35 mm glass-bottomed dishes at a density of 2.5×10^5 cells/dish and exposed to 300 μM Fe-NTA the following day, the medium was replaced

with fresh medium containing the same component every 24 h. In some cases, cells were treated with Ru360 for 1 h prior to Fe-NTA treatment. After five days, the cell culture medium was replaced with phenol red-free DMEM containing Fe-NTA and Ru360, and the dish was protected from light. The following day, spontaneous CL was measured using a single photoelectron counting system (CLD-10; Tohoku Electronic Industrial Co., Ltd., Sendai, Japan), as described previously (Maeda et al., 2010). Emission was expressed in counts/10 min/mg protein.

ROS production was also assessed using HPF as a fluorescent probe for the selective detection of hydroxyl radicals. Briefly, cells were seeded into 35 mm glass-bottomed dishes, as described for CL analysis. After 7 days, the cell culture medium was replaced with modified Hanks' balanced salt solution (HBSS) containing 10 mM HEPES, 1 mM $MgCl_2$, 2 mM $CaCl_2$ and 2.7 mM glucose (pH 7.4). Next, 10 μM HPF and 20 nM MitoTracker® Red (a fluorescent probe for the mitochondria) were added, and cells were incubated for 15 min at 37 °C. Images of HPF and MitoTracker® Red staining were obtained using a laser scanning confocal microscope (FV300; Olympus Optical Co., Ltd., Tokyo, Japan). The wavelengths (excitation/emission) for the detection of HPF (green) and MitoTracker® Red (red) were 488 nm/515 nm and 579 nm/599 nm, respectively.

Assessment of mitochondrial membrane potential. Measurement of mitochondrial membrane potential was performed using the JC-1 stain, a lipophilic cation fluorescent dye that accumulates in the mitochondria. At a low mitochondrial membrane potential, the JC-1 dye exists as a monomeric molecule and fluoresces green, whereas at a higher membrane potential the JC-1 dye forms polymeric aggregates and fluoresces red. A fall in the mitochondrial membrane potential is therefore indicated by a decrease in the ratio of red signal to green signal.

Cells were cultured in 96 well black culture plates at a density of 8.4×10^3 cells/well and exposed to various concentrations of Fe-NTA the following day, the medium was replaced with fresh medium containing the same component every 24 h. After six days, the culture medium was replaced with 200 μl JC-1 solution (10 μg/ml JC-1 in HBSS), and cells were incubated in the dark for 30 min at 37 °C. After washing twice with HBSS, the absorbance of the cells in each well was immediately measured using a fluorescence plate reader with the excitation and emission wavelengths set at 490 nm and 530 nm (green)/590 nm (red), respectively.

Animals. The production of transgenic mice expressing the HCV core protein has been described previously (Moriya et al., 2001). Briefly, the HCV core protein gene was placed downstream of a transcriptional regulatory region from the hepatitis B virus and introduced into C57BL/6 mouse embryos (Clea Japan, Tokyo, Japan). All of the animals were treated humanely in accordance with the guidelines issued by the National Institute of Health and all procedures described below were approved by the animal care committee of Chiba University.

Isolation of mouse liver mitochondria. The mouse liver mitochondrial fraction was prepared according to a previously described method (Masubuchi et al., 2002). Livers were isolated from two mice and placed in ice-cold buffer containing 250 mM sucrose, 10 mM HEPES–KOH, and 0.5 mM EGTA (pH 7.4). Livers were cut into small cubes with scissors in the same buffer and homogenized five times with a Potter homogenizer. The homogenates were diluted to 0.25 g liver/ml and were centrifuged at 770 ×g for 5 min at 4 °C. The resulting supernatant was decanted and further centrifuged at 9800 ×g for 10 min. The pellet was resuspended to yield a concentration of 0.5 g liver/ml in buffer containing 250 mM sucrose, 10 mM HEPES–KOH and 0.3 mM EGTA (pH 7.4), and centrifuged at 4500 ×g for 10 min. The pellet was resuspended to yield a concentration of 1 g liver/ml in the same buffer and centrifuged at 2000 ×g for 2 min, followed by further centrifugation at 4500 ×g for 8 min. The

final pellet was then resuspended in buffer containing 250 mM sucrose and 10 mM HEPES–KOH (pH 7.4) and used for further experiments.

Mitochondrial iron uptake. All experiments were conducted in a 30 °C water bath. After pre-incubation of the mitochondria in buffer containing 225 mM sucrose, 10 mM KCl, 5 mM $MgCl_2$, 5 mM KH_2PO_4, and 20 mM Tris–HCl (pH 7.4) for 1 min, Ru360 was added at a final concentration of 10 µM, $^{59}FeSO_4$ was added after 1 min, and the ^{59}Fe remaining in the mitochondria after 10 min was measured using a gamma counter.

Western blotting analysis. The mouse liver mitochondrial fraction (10 µg protein) was subjected to electrophoresis on a 12.5% polyacrylamide slab gel containing 0.1% sodium dodecyl sulfate and transferred onto an Immobilon-P Transfer Membrane filter (Millipore Corporation, Billerica, MA). The membrane was blocked for 1 h at room temperature with Tris-buffered saline/0.05% Tween 20 (TTBS) containing 3% bovine serum albumin (BSA) and probed overnight at 4 °C with the CCDC109A goat polyclonal IgG (1:200) against the Ca^{2+} uniporter and the ANT goat polyclonal IgG (1:1000). The membrane was then incubated for 1 h at room temperature with donkey anti-goat IgG-HRP (1:3333). All antibodies were diluted in TTBS containing 0.1% BSA. Immunoreactive bands were detected using a LAS-1000 imaging system (Fuji Film, Tokyo, Japan) and an enhanced CL system (GE Healthcare, Little Chalfont, Buckinghamshire, UK).

Statistical analysis. All data are represented as the mean ± the standard error (S.E.). Data were statistically analyzed by using one-way ANOVA followed by the Bonferroni test for multiple comparison. For comparison among two groups, two-tailed Student's t-test was adopted. Differences between means at the level of P < 0.05 were considered significant.

Results

Iron-induced cytotoxicity in HCV core protein-expressing HepG2 cells

The iron uptake system is perturbed in HCV-infected hepatocytes due to elevated expression of transferrin receptor 1. However, because of its hydrophobicity, Fe-NTA is taken up into the cell in a transferrin receptor 1-independent manner by passive diffusion. Fe-NTA is then converted into free Fe^{2+} by several types of esterases. Therefore, Fe-NTA was used in the current study to control for intrinsic differences in active iron uptake between HCV core protein-expressing HepG2 cells (Hep39b cells) and vector-transfected HepG2 cells (Hepswx cells). After treatment with Fe-NTA for six days, cytotoxicity was assessed using the MTT assay. Concentration-dependent cytotoxicity of Fe-NTA against Hep39b cells was observed. By contrast, no cytotoxicity was observed against control Hepswx cells at Fe-NTA concentrations of less than 1000 µM (Fig. 1). These data indicate that HCV core protein expression affects the susceptibility of hepatocytes to Fe-NTA-induced iron cytotoxicity.

Effect of iron accumulation on ROS production in HCV core protein-expressing versus control hepatocytes

To directly measure free radical formation, we took advantage of methodology for measuring spontaneous CL and compared the levels of CL in HCV core protein-expressing Hep39b and control Hepswx cells (Fig. 2a). As shown in Fig. 2a, spontaneous CL was significantly higher in Hep39b cells by approximately 156% compared with that in Hepswx cells (6015 versus 3856 arbitrary units; P < 0.01). In the presence of 300 µM Fe-NTA, iron-induced CL was also significantly higher in Hep39b cells relative to Hepswx cells (2.61-fold versus 1.54-fold increase; P < 0.01 and P < 0.001, respectively) (Fig. 2a).
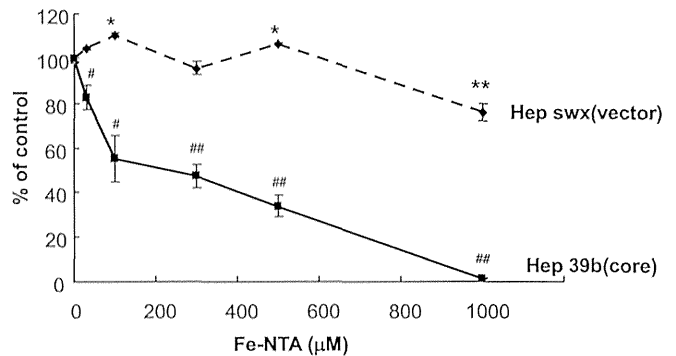

Fig. 1. Iron-induced cytotoxicity in control versus HCV core protein-expressing hepatocytes. Hepswx (dashed line) and Hep39b (solid line) cells were exposed with Fe-NTA (30, 100, 300, 500 and 1000 µM) for six days. Hepatotoxicity was determined using the MTT assay. Viability was calculated as the absorbance of the experimental sample relative to that of the controls (without Fe-NTA treatments). Values are the mean ± the S.E. *P < 0.05 and **P < 0.01, significantly different from the control (without Fe-NTA). #P < 0.05 and ##P < 0.01, significantly different from respective control cells (Hepswx) (n = 6).

Effect of iron accumulation on mitochondrial ROS production

Mitochondria are a major source of ROS production. Therefore, we next examined the production of mitochondrial hydroxyl radicals by free iron catalyzation (i.e., the Fenton reaction). Since increased production of ROS was observed in Hep39b cells in the presence of Fe-NTA, we next examined mitochondrial ROS production by double staining with MitoTracker® Red (red), a fluorescent probe for the mitochondria, and HPF (green), a fluorescent probe for the selective detection of hydroxyl radicals. As shown in Fig. 2b, a strong fluorescent signal derived from HPF was observed in Hep39b cells in the presence of Fe-NTA. This fluorescence overlapped with that generated by MitoTracker® Red (Fig. 2b). The fluorescent signal derived from HPF in overlapped area was significantly higher in Hep39b cells by approximately 200% compared with that in Hepswx cells (Fig. 2c). These data indicate that mitochondrial hydroxyl radical production was increased in the presence of the HCV core protein and Fe-NTA.

Effect of HCV core protein on mitochondrial membrane potential

The HCV core protein is known to inhibit mitochondrial respiratory complex I activity (Korenaga et al., 2005). Inhibition of complex I leads to ROS formation due to premature electron leakage from the complex. Therefore, we next examined the effect of Fe-NTA on mitochondrial membrane potential in Hep39b cells by using JC-1, a lipophilic cationic dye that selectively enters the mitochondria and reversibly changes color from green to red as the membrane potential increases. Fig. 3 demonstrates that the mitochondrial membrane potential was decreased in HCV core protein-expressing Hep39b cells compared with control Hepswx cells. The decrease in membrane potential was significantly increased following exposure to Fe-NTA (300 and 1000 µM) for six days (Fig. 3).

Mitochondrial free iron uptake in HCV core protein-expressing versus control hepatocytes

Because mitochondrial hydroxyl radical production was increased in the presence of Fe-NTA (Fig. 2), the uptake of free iron into isolated mitochondria was next examined. To ensure a sufficient quantity and quality of the mitochondria for this experiment, mitochondria were isolated from the liver of HCV core protein-expressing transgenic and wild-type (control) mice. Fig. 4 shows that the concentration of mitochondrial free
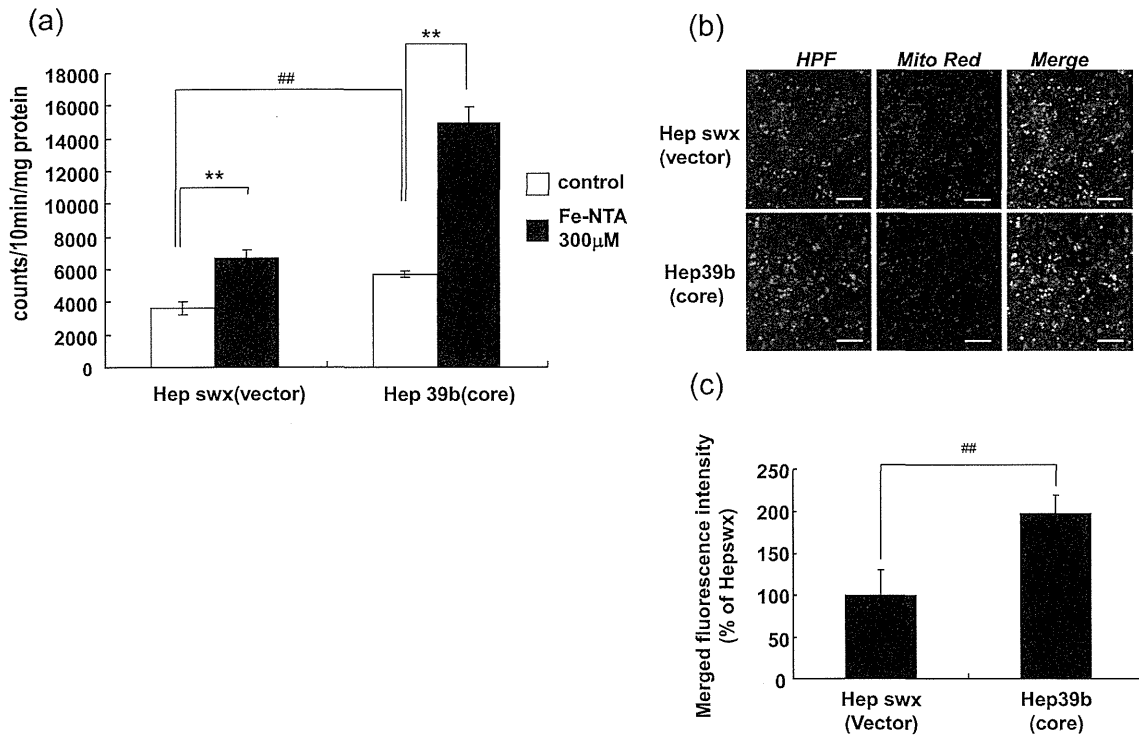
(a)

(b)

(c)

Fig. 2. Iron-induced mitochondrial ROS production is enhanced in HCV core protein-expressing hepatocytes. (a) Hepswx and Hep39b cells were exposed to Fe-NTA (300 µM) for six days. ROS production was determined using a CL analyzer. Detected counts were normalized by protein content of cell lysate. Values are given as the mean ± the S.E. **P < 0.01 and ##P < 0.01, significantly different from respective control (n = 3–4). (b) Hepswx and Hep39b cells were pretreated with HPF (green) and MitoTracker® Red (red). Mitochondrial ROS production was determined by the strength of yellow fluorescence in the merged pictures. The scale bar represents 100 µm. (c) Analysis of merged fluorescence microscopy images was done by ImageJ. Integrated density of merged area was automatically selected and fluorescence intensity of HPF was calculated within the merged area of 200–300 cells.

iron ($^{59}Fe^{2+}$) was significantly increased in the mitochondria derived from the transgenic versus the control mouse liver (62.2 ± 4.2 versus 79.5 ± 2.1 pmol/mg protein, respectively; P < 0.05), whereas the passive diffusion of $^{59}Fe^{2+}$ into the mitochondria (estimated by $^{59}Fe^{2+}$ uptake at 4 °C) was 31.1 ± 3.2 pmol/10 min/mg protein in Hepswx cells, and 29.2 ± 1.8 pmol/10 min/mg protein in Hep39b cells (not significantly different). Moreover, $^{59}Fe^{2+}$ uptake into the transgenic and control mitochondria was attenuated to the same level by Ru360 (48.2 ± 4.1 versus 47.5 ± 1.2 pmol/mg protein, respectively) (Fig. 4). These

data indicate that calcium uniporter plays a role in free iron uptake into the mitochondria and that the activity of the Ca^{2+} uniporter is increased by the HCV core protein.

Effect of Ru360 on Fe-NTA-induced ROS production and cytotoxicity

We next examined the effect of Ru360 on Fe-NTA-induced ROS production and cytotoxicity in Hep39b versus Hepswx cells. As shown in Fig. 5a, in the absence of Fe-NTA, Ru360 had no effect on ROS production
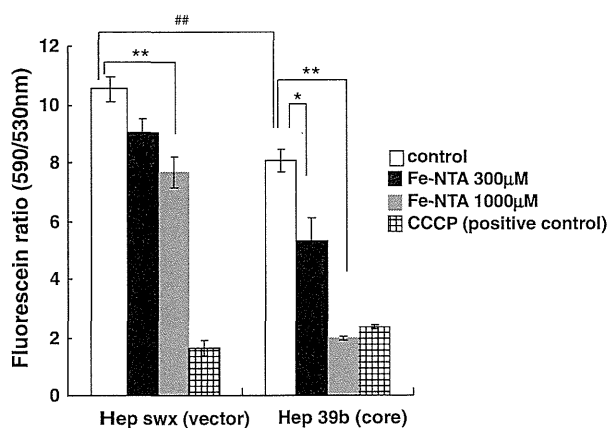
Fig. 3. The iron-induced reduction in mitochondrial membrane potential is increased by the expression of HCV core protein. Hepswx and Hep39b cells were exposed to Fe-NTA for six days. Mitochondrial membrane potential was estimated fluorometrically. Values are given as the mean ± the S.E. *P < 0.05, **P < 0.01 and ##P < 0.01, significantly different from respective control (n = 6).

Fig. 4. Mitochondrial iron uptake is augmented by the expression of HCV core protein and inhibited by Ru360. Mitochondria were isolated from wild-type and HCV core protein transgenic (Tg) mice and exposed to $^{59}FeSO_4$ with/without Ru360. Free iron uptake was measured in the isolated mitochondria and the free iron uptake amount was normalized by mitochondrial protein content. The dashed line represents the passive diffusion into the mitochondria. Values are given as the mean ± the S.E. **P < 0.01 and #P < 0.05, significantly different from respective control (n = 3–8).

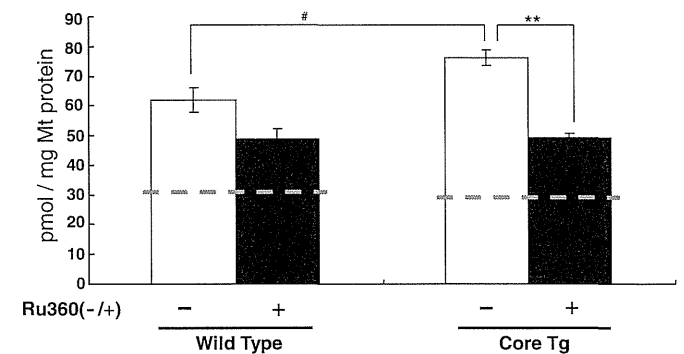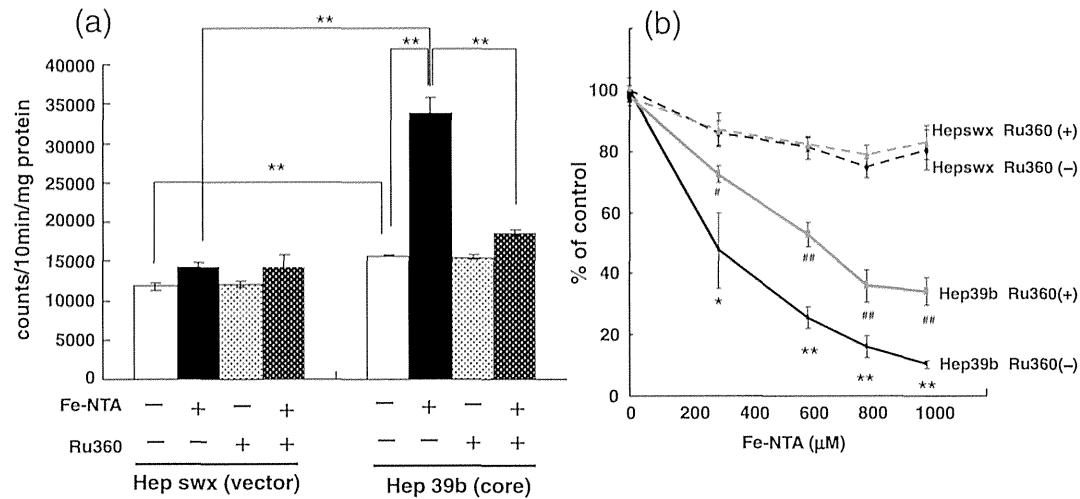**Fig. 5.** Iron-induced ROS production and cytotoxicity are inhibited by Ru360 in HCV core protein-expressing hepatocytes. (a) Hepswx and Hep39b cells were exposed to Fe-NTA (300 μM) and Ru360 (20 μM) for six days. ROS production was determined using a CL analyzer. Values are given as the mean ± the S.E. **P < 0.01, significantly different from respective control (n = 8). (b) Hepswx and Hep39b cells were exposed to Fe-NTA (300, 600, 800, and 1000 μM) and Ru360 (20 μM) for six days. Cytotoxicity was determined using the MTT assay. Values are given as the mean ± the S.E. *P < 0.05 and **P < 0.01, significantly different from Hepswx Ru360(−). #P < 0.05 and ##P < 0.01, significantly different from Hep39b Ru360(−) (n = 6).

in Hepswx cells and Hep39b cells. On the other hand, Ru360 significantly suppressed Fe-NTA (300 μM)-induced ROS production in Hep39b but not Hepswx cells (Fig. 5a). Moreover, cytotoxicity following exposure to (300, 600, 800 and 1000 μM) Fe-NTA for six days was also specifically inhibited by Ru360 treatment in Hep39b cells (Fig. 5b).

Expression of the Ca^{2+} uniporter in isolated mitochondria

Given that mitochondrial free iron uptake is enhanced in HCV core protein-expressing Hep39b cells (Fig. 4), we next examined the expression of the Ca^{2+} uniporter in the mitochondria isolated from the liver of HCV core protein-expressing transgenic mice relative to control mice. As shown in Fig. 6, mitochondrial expression of the uniporter was similar in transgenic versus control mice, as assessed by Western blot analysis.
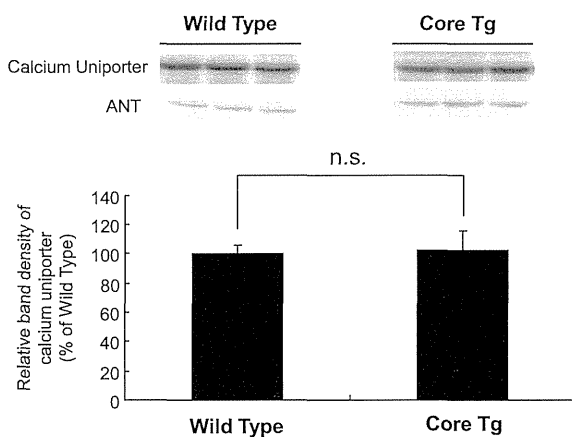

Fig. 6. Expression of mitochondrial Ca^{2+} uniporter in the livers of HCV core protein-expressing transgenic versus wild-type mice. Mitochondria were isolated from the livers of wild-type (control) and HCV core protein-expressing transgenic (Tg) mice. The expression levels of the Ca^{2+} uniporter and ANT (loading control) were determined by Western blot analysis. Mitochondrial proteins (10 μg) were loaded into each lane of the gel. The band density of the uniporter was normalized to the band density of ANT. Values are given as the mean ± the S.E. n.s.: not significantly different (n = 3).

Discussion

The accumulation of iron into the liver of HCV core protein-expressing transgenic mice fed a normal diet is similar to that observed in chronic HCV patients (Farinati et al., 1995; Kato et al., 2001). On the other hand, the expression level of hepcidin, which regulates iron metabolism by inhibiting iron absorption from the intestine and the hepatic portal system, is reportedly decreased in the liver of HCV patients and full-length HCV genome-expressing transgenic mice, but not in the liver of HCV core protein-expressing transgenic mice (Moriya et al., 2010; Muckenthaler, 2008). Therefore, although the precise regulation of iron transport into the mitochondria is essential for heme biosynthesis, hemoglobin production, and Fe–S clustering, the mechanism(s) behind mitochondrial iron homeostasis is not yet fully understood.

Previous work from our group revealed elevated ROS generation in HCV core protein-expressing transgenic mice (Moriya et al., 2001). Moreover, our previous work, along with that of others (Korenaga et al., 2005), showed that the core protein interacts with the outer mitochondrial membrane and impairs the mitochondrial respiratory chain in the normal mouse liver via inhibition of complex I activity (unpublished data). Inhibition of respiratory chain complexes ultimately leads to the overproduction of ROS via electron leakage from the mitochondria. Therefore, we hypothesized that the inducible mitochondrial iron transport system exacerbates hepatic toxicity caused by the HCV core protein.

This study employed Fe-NTA to exclude intrinsic differences in iron uptake into HCV core protein-expressing Hep39b cells and vector-transfected Hepswx cells. In addition, we demonstrated that HCV core protein-induced alterations in mitochondrial ROS production and membrane potential were augmented in the presence of iron (Figs. 2 and 3). These data may indicate that iron-dependent mitochondrial dysfunction was amplified via the Fenton reaction, which produces potent reactive free radicals (i.e., hydroxyl radicals) (Fig. 7).

Iron is absolutely essential for the sustenance of all forms of life due to its unusual ability to serve as both an electron donor and acceptor. On the other hand, free iron is also potentially toxic, which is related to its ability to donate and accept electrons within the cell. Free iron catalyzes the conversion of hydrogen peroxide into free radicals, which can cause damage to the mitochondria and cellular structures. For this reason, the iron homeostasis is strictly regulated, and the impairment of iron homeostasis is related to several diseases. In patients with HCV, hepatic
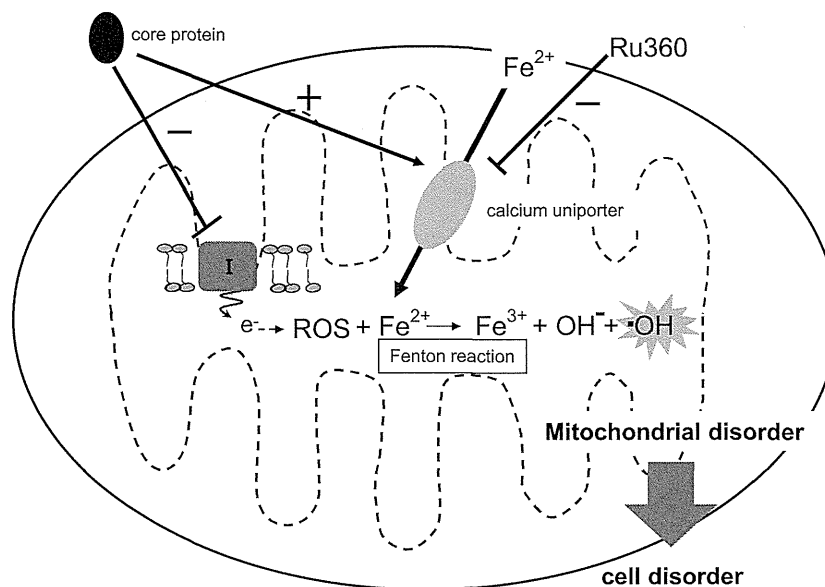
Fig. 7. Proposed mechanism of mitochondrial iron accumulation and hepatic cytotoxicity caused by the HCV core protein. The HCV core protein induces mitochondrial ROS production by inhibiting mitochondrial complex I. In addition, it is suggested that the HCV core protein stimulates mitochondrial iron uptake through the mitochondrial Ca^{2+} uniporter. The excess iron then leads to mitochondrial ROS production and mitochondrial/cellular malfunction/disorder when the HCV core protein is expressed.

and serum free iron concentrations are ~7-fold higher (12.5 mmol/g liver and 134 mg/dl, respectively) than those of a normal individual (Farinati et al., 1995; Kageyama et al., 1998; Olynyk et al., 1995; Silva et al., 2005). In this study, significant hepatotoxicity was observed at 30 μM Fe-NTA in HCV core protein-expressing Hep39b cells (Fig. 1). Therefore, a physiologically relevant concentration of iron (30 μM), which is not sufficient to induce cell toxicity by itself, was synergistic with the toxic actions of the core protein (Fig. 1). This interplay was similarly revealed by the synergy between iron and the core protein in inducing mitochondrial dysfunction and ROS production (Figs. 2 and 3).

This study further demonstrated that mitochondrial free iron uptake was partially mediated by the Ca^{2+} uniporter. The Ca^{2+} uniporter was selectively inhibited by Ru360 and exhibited an increased capacity to uptake iron into HCV core protein-expressing liver mitochondria versus normal liver mitochondria (Fig. 4). However, the expression of the uniporter was unaltered in core protein-expressing transgenic mice relative to normal mice (Fig. 6). Li et al. (2007) reported that the activity of the Ca^{2+} uniporter was up-regulated in the presence of the core protein: The in vitro incubation of mouse liver mitochondria with HCV core protein (100 ng/mg) increased the Ca^{2+} entry rate by ~2-fold. The Ca^{2+} uniporter is located in the inner mitochondrial membrane and transports not only Ca^{2+} but also other metal cationic ions (e.g., Fe^{2+}) into the mitochondrial matrix space in a mitochondrial membrane potential-dependent fashion (Bernardi, 1999).

Iron uptake was significantly suppressed to the same level by Ru360 in the mitochondria isolated from both core protein-expressing transgenic and normal mice (Fig. 4). Moreover, as free iron uptake into the mitochondria was still observed at 4 °C for both types of the mitochondria, about half of the iron (Hepswx; 31.1 ± 3.2 pmol/10 min/mg protein, Hep39b; 29.2 ± 1.8 pmol/10 min/mg protein) was estimated to enter into the mitochondria by passive diffusion (Fig. 4, dashed line). These data indicate that the up-regulation of iron uptake in the mitochondria isolated from transgenic mice was mediated by the HCV core protein-induced stimulation of Ru360-sensitive Ca^{2+} uniporter transport activity. However, the mechanism by which the core protein alters the function of the mitochondrial uniporter is still unclear, especially given that the core protein binds to the outer mitochondrial membrane, and the uniporter is located in the inner mitochondrial membrane. It is known that mitochondrial calcium uniporter possibly

forms multi-molecular complex (Raffaello et al., 2012). Mitochondrial calcium uniporter function could be altered by the effect on essential regulator and/or protein involved in the assembly of the channel. In this regard, though our current study demonstrated that HCV core protein had no effect on Ca^{2+} uniporter expression (Fig. 6), it is possible that other mechanisms are involved in the HCV core protein-induced stimulation of Ca^{2+} uniporter transport activity. Further study should be addressed in the future.

Interferon-α has been used as monotherapy for chronic hepatitis C, yet only about 40–50% of hepatitis C patients experience an initial biochemical response to the cytokine. Interestingly, high iron accumulation in chronic HCV carriers is related to a poor response to interferon therapy (Walters et al., 1973). In addition, some investigators have suggested that iron removal therapy (via phlebotomy or food therapy (i.e., restriction of an iron rich-diet)) can attenuate liver damage in hepatitis C patients by still unknown mechanisms (Hayashi et al., 1994; Kato et al., 2007). The current study showed that the HCV core protein-induced mitochondrial iron uptake is responsible for exacerbating mitochondrial dysfunction and ROS production, which finally seems to lead to hepatocyte toxicity (Fig. 7). Based on these results, we suggest that inhibition of the mitochondrial Ca^{2+} uniporter may provide a new therapeutic approach to treat liver disease in HCV patients.

Conflict of interest statement

The authors declare no conflict of interest.

Acknowledgments

References

Awai, M., Narasaki, M., Yamanoi, Y., Seno, S., 1979. Induction of diabetes in animals by parenteral administration of ferric nitrilotriacetate. A model of experimental hemochromatosis. Am. J. Pathol. 95, 663–673.

72

Bartenschlager, R., Lohmann, V., 2000. Replication of hepatitis C virus. J. Gen. Virol. 81, 1631–1648.

Bernardi, P., 1999. Mitochondrial transport of cations: channels, exchangers, and permeability transition. Physiol. Rev. 79, 1127–1155.

Bonkovsky, H.L., Banner, B.F., Rothman, A.L., 1997. Iron and chronic viral hepatitis. Hepatology 25, 759–768.

Bukh, J., Miller, R.H., Purcell, R.H., 1995. Genetic heterogeneity of hepatitis C virus: quasispecies and genotypes. Semin. Liver Dis. 15, 41–63.

Choi, J., Ou, J.H., 2006. Mechanisms of liver injury. III. Oxidative stress in the pathogenesis of hepatitis C virus. Am. J. Physiol. Gastrointest. Liver Physiol. 290, G847–G851.

Farinati, F., Cardin, R., De Maria, N., Della Libera, G., Marafin, C., Lecis, E., et al., 1995. Iron storage, lipid peroxidation and glutathione turnover in chronic anti-HCV positive hepatitis. J. Hepatol. 22, 449–456.

Hayashi, H., Takikawa, T., Nishimura, N., Yano, M., Isomura, T., Sakamoto, N., 1994. Improvement of serum aminotransferase levels after phlebotomy in patients with chronic active hepatitis C and excess hepatic iron. Am. J. Gastroenterol. 89, 986–988.

Ikeda, K., Saitoh, S., Suzuki, Y., Kobayashi, M., Tsubota, A., Koida, I., et al., 1998. Disease progression and hepatocellular carcinogenesis in patients with chronic viral hepatitis: a prospective observation of 2215 patients. J. Hepatol. 28, 930–938.

Kageyama, F., Kobayashi, Y., Murohisa, G., Shimizu, E., Suzuki, F., Kikuyama, M., et al., 1998. Failure to respond to interferon-alpha 2a therapy is associated with increased hepatic iron levels in patients with chronic hepatitis C. Biol. Trace Elem. Res. 64, 185–196.

Kato, J., Kobune, M., Nakamura, T., Kuroiwa, G., Takada, K., Takimoto, R., et al., 2001. Normalization of elevated hepatic 8-hydroxy-2′-deoxyguanosine levels in chronic hepatitis C patients by phlebotomy and low iron diet. Cancer Res. 61, 8697–8702.

Kato, J., Miyanishi, K., Kobune, M., Nakamura, T., Takada, K., Takimoto, R., et al., 2007. Long-term phlebotomy with low-iron diet therapy lowers risk of development of hepatocellular carcinoma from chronic hepatitis C. J. Gastroenterol. 42, 830–836.

Korenaga, M., Wang, T., Li, Y., Showalter, L.A., Chan, T., Sun, J., et al., 2005. Hepatitis C virus core protein inhibits mitochondrial electron transport and increases reactive oxygen species (ROS) production. J. Biol. Chem. 280, 37481–37488.

Kowdley, K.V., 2004. Iron, hemochromatosis, and hepatocellular carcinoma. Gastroenterology 127, S79–S86.

Lau, J.Y., Xie, X., Lai, M.M., Wu, P.C., 1998. Apoptosis and viral hepatitis. Semin. Liver Dis. 18, 169–176.

Li, Y., Boehning, D.F., Qian, T., Popov, V.L., Weinman, S.A., 2007. Hepatitis C virus core protein increases mitochondrial ROS production by stimulation of Ca^{2+} uniporter activity. FASEB J. 21, 2474–2485.

Maeda, T., Miyazono, Y., Ito, K., Hamada, K., Sekine, S., Horie, T., 2010. Oxidative stress and enhanced paracellular permeability in the small intestine of methotrexate-treated rats. Cancer Chemother. Pharmacol. 65, 1117–1123.

Masubuchi, Y., Nakayama, S., Horie, T., 2002. Role of mitochondrial permeability transition in diclofenac-induced hepatocyte injury in rats. Hepatology 35, 544–551.

Moriya, K., Nakagawa, K., Santa, T., Shintani, Y., Fujie, H., Miyoshi, H., et al., 2001. Oxidative stress in the absence of inflammation in a mouse model for hepatitis C virus-associated hepatocarcinogenesis. Cancer Res. 61, 4365–4370.

Moriya, K., Miyoshi, H., Shinzawa, S., Tsutsumi, T., Fujie, H., Goto, K., et al., 2010. Hepatitis C virus core protein compromises iron-induced activation of antioxidants in mice and HepG2 cells. J. Med. Virol. 82, 776–792.

Muckenthaler, M.U., 2008. Fine tuning of hepcidin expression by positive and negative regulators. Cell Metab. 8, 1–3.

Nishioka, K., Watanabe, J., Furuta, S., Tanaka, E., Iino, S., Suzuki, H., et al., 1991. A high prevalence of antibody to the hepatitis C virus in patients with hepatocellular carcinoma in Japan. Cancer 67, 429–433.

Oberley, T.D., 2002. Oxidative damage and cancer. Am. J. Pathol. 160, 403–408.

Okuda, M., Li, K., Beard, M.R., Showalter, L.A., Scholle, F., Lemon, S.M., et al., 2002. Mitochondrial injury, oxidative stress, and antioxidant gene expression are induced by hepatitis C virus core protein. Gastroenterology 122, 366–375.

Olynyk, J.K., Reddy, K.R., Di Bisceglie, A.M., Jeffers, L.J., Parker, T.I., Radick, J.L., et al., 1995. Hepatic iron concentration as a predictor of response to interferon alfa therapy in chronic hepatitis C. Gastroenterology 108, 1104–1109.

Otani, K., Korenaga, M., Beard, M.R., Li, K., Qian, T., Showalter, L.A., et al., 2005. Hepatitis C virus core protein, cytochrome P450 2E1, and alcohol produce combined mitochondrial injury and cytotoxicity in hepatoma cells. Gastroenterology 128, 96–107.

Park, J.S., Yang, J.M., Min, M.K., 2000. Hepatitis C virus nonstructural protein NS4B transforms NIH3T3 cells in cooperation with the Ha-ras oncogene. Biochem. Biophys. Res. Commun. 267, 581–587.

Raffaello, A., De Stefani, D., Rizzuto, R., 2012. The mitochondrial Ca^{2+} uniporter. Cell Calcium 52, 16–21.

Ray, R.B., Meyer, K., Ray, R., 2000. Hepatitis C virus core protein promotes immortalization of primary human hepatocytes. Virology 271, 197–204.

Silva, I.S., Perez, R.M., Oliveira, P.V., Cantagalo, M.I., Dantas, E., Sisti, C., et al., 2005. Iron overload in patients with chronic hepatitis C virus infection: clinical and histological study. J. Gastroenterol. Hepatol. 20, 243–248.

Walters, G.O., Miller, F.M., Worwood, M., 1973. Serum ferritin concentration and iron stores in normal subjects. J. Clin. Pathol. 26, 770–772.

Wang, T., Weinman, S.A., 2006. Causes and consequences of mitochondrial reactive oxygen species generation in hepatitis C. J. Gastroenterol. Hepatol. 21 (Suppl. 3), S34–S37.

Wang, T., Campbell, R.V., Yi, M.K., Lemon, S.M., Weinman, S.A., 2010. Role of hepatitis C virus core protein in viral-induced mitochondrial dysfunction. J. Viral Hepat. 17, 784–793.

World Journal of Gastroenterology

CASE REPORT

Acute hepatitis B of genotype H resulting in persistent infection

Norie Yamada, Ryuta Shigefuku, Ryuichi Sugiyama, Minoru Kobayashi, Hiroki Ikeda, Hideaki Takahashi, Chiaki Okuse, Michihiro Suzuki, Fumio Itoh, Hiroshi Yotsuyanagi, Kiyomi Yasuda, Kyoji Moriya, Kazuhiko Koike, Takaji Wakita, Takanobu Kato

Norie Yamada, Ryuichi Sugiyama, Takaji Wakita, Takanobu Kato, Department of Virology II, National Institute of Infectious Diseases, Shinjyuku-Ku, Tokyo 162-8640, Japan
Norie Yamada, Minoru Kobayashi, Kiyomi Yasuda, Department of Internal Medicine, Center for Liver Diseases, Kiyokawa Hospital, Suginami, Tokyo 166-0004, Japan
Norie Yamada, Ryuta Shigefuku, Minoru Kobayashi, Hiroki Ikeda, Hideaki Takahashi, Chiaki Okuse, Michihiro Suzuki, Fumio Itoh, Division of Gastroenterology and Hepatology, Department of Internal Medicine, St. Marianna University School of Medicine, Kanagawa 216-8511, Japan
Hiroshi Yotsuyanagi, Department of Infectious Diseases, Graduate School of Medicine, The University of Tokyo, Tokyo 113-8655, Japan
Kyoji Moriya, Department of Infection Control and Prevention, Graduate School of Medicine, The University of Tokyo, Tokyo 113-8655, Japan
Kazuhiko Koike, Department of Gastroenterology, Graduate School of Medicine, The University of Tokyo, Tokyo 113-8655, Japan
Author contributions: Shigefuku R, Kobayashi M, Ikeda H, Takahashi H, Okuse C, Suzuki M and Itoh F were the patient's attending physicians; Yotsuyanagi H, Yasuda K, Moriya K, Koike K, Wakita T and Kato T organized the study; Yamada N, Sugiyama R and Kato T performed the research; Yamada N and Kato T wrote the manuscript.
Supported by Japan Society for the Promotion of Science and the Ministry of Health, Labour and Welfare and the Ministry of Education, Culture, Sports, Science and Technology of Japan
Correspondence to: Takanobu Kato, MD, PhD, Department of Virology II, National Institute of Infectious Diseases, Toyama 1-23-1, Shinjyuku-Ku, Tokyo 162-8640, Japan. takato@nih.go.jp
Telephone: +81-3-52851111 Fax: +81-3-52851161
Received: October 3, 2013   Revised: November 18, 2013
Accepted: December 5, 2013
Published online: March 21, 2014

Abstract

A 47-year-old man presented with general fatigue and dark urine. The laboratory data showed increased levels of hepatic transaminases. The patient was positive for hepatitis B virus (HBV) markers and negative for anti-human immunodeficiency virus. The HBV-DNA titer was set to 7.7 log copies/mL. The patient was diagnosed with acute hepatitis B. The HBV infection route was obscure. The serum levels of hepatic transaminases decreased to normal ranges without any treatment, but the HBV-DNA status was maintained for at least 26 mo, indicating the presence of persistent infection. We isolated HBV from the acute-phase serum and determined the genome sequence. A phylogenetic analysis revealed that the isolated HBV was genotype H. In this patient, the elevated peak level of HBV-DNA and the risk alleles at human genome single nucleotide polymorphisms s3077 and rs9277535 in the human leukocyte antigen-DP locus were considered to be risk factors for chronic infection. This case suggests that there is a risk of persistent infection by HBV genotype H following acute hepatitis; further cases of HBV genotype H infection must be identified and characterized. Thus, the complete determination of the HBV genotype may be essential during routine clinical care of acute hepatitis B outpatients.

Core tip: Hepatitis B virus (HBV) genotype H infection is rare in Asia, particularly in Japan. Here, we report a case of acute hepatitis B caused by a genotype H strain with persistent infection, although most adult cases of acute hepatitis B are self-limiting in Japan. This case suggests that the HBV genotype H infection can be a risk factor for persistent infection. Therefore, it is necessary to investigate the characteristics of genotype H infection in an accumulation of cases. Thus, the

complete determination of the HBV genotype may be essential in the routine clinical care of acute hepatitis B patients.

INTRODUCTION

Hepatitis B is a potentially life-threatening liver infection caused by the hepatitis B virus (HBV); it represents a major global health problem. HBV can cause chronic liver diseases and increases the risk of death from cirrhosis and liver cancer. Worldwide, an estimated two billion people have been infected with HBV and more than 240 million have chronic infections[1]. The HBV genome consists of approximately 3200-nucleotides of DNA; the virus replicates using a reverse transcriptase enzyme that lacks proofreading ability. Therefore, HBV possesses diverse genetic variability, and the viral population is classified into at least eight genotypes that are designated A -H[2-6]. In Japan, genotypes B and C are prevalent among patients with chronic infections. However, in the last decades, the prevalent genotype in acute HBV infections has shifted from genotype C to A[7-9]. There are some differences in the clinical features and outcomes among the genotypes[10-13]. It has been reported that the persistent infection from acute hepatitis is prevalent in adults that are infected with genotype A HBV. Thus, determining the HBV genotype is of increasing importance even in routine clinical practice, although a reliable kit for determination of all HBV genotypes is still uncommon and is not yet covered by insurance. The host factors associated with persistent infection by HBV have also been reported, such as single nucleotide polymorphisms (SNPs) or genotypes in the human leukocyte antigen-DP locus. It may also be useful for identifying the patients who are prone to develop chronic hepatitis.

In this report, we describe a case of acute hepatitis B resulting from infection by a genotype H strain of HBV. Although the laboratory data and symptoms were not distinguishable from acute hepatitis B with other genotypes, this patient developed persistent infection.

CASE REPORT

A 47-year-old man living in Kawasaki, Japan, presented at our hospital with general fatigue and dark urine. Approximately 1 wk before visiting the hospital, the patient developed nausea, loss of appetite, and a feeling of fullness in the abdomen. Four days later, he noted darkening of his skin and urine. Upon admission, the patient's laboratory data revealed elevated serum aspartate aminotransferase, alanine aminotransferase (ALT), lactate dehydrogenase, alkaline phosphatase, γ-glutamylt ranspeptidase, and total bilirubin (T-Bil) levels (Table 1). The prothrombin activity was within the normal range (95%). Test for hepatitis B surface antigen (HBsAg; HISCL-2000i, Sysmex, Kobe, Hyogo, Japan), hepatitis B e-antigen (HBeAg; ARCHITECT® CLIA, Abbott Japan, Tokyo, Japan) and anti-hepatitis B core antigen (anti-HBc) IgM (ARCHITECT® CLIA) were positive. A test for HBV-DNA was also positive, exhibiting a titer of 7.7 log copies/mL (COBAS TaqMan HBV Test v2.0, Roche Diagnostics, Tokyo, Japan). HBsAg had not been detected 2 years previously when the patient had been admitted to another hospital for treatment of acute enterocolitis. Other hepatitis virus markers were negative. Therefore, the patient was diagnosed with acute hepatitis B. The genotype of the infecting HBV, as assessed by the Immunis HBV Genotype Immunis® HBV Genotype EIA Kit (Institute of Immunology, Tokyo, Japan), was determined as genotype C. The patient had not been abroad in the past 12 mo; he had no history of receiving blood or blood-related products, transfusions, or drug injections, and he reported no personal or family history of liver disease. The man was unmarried and declared that he was heterosexual, with no history of sexual contact with commercial sex workers or strangers. Anti-human immunodeficiency virus (HIV) was not detected. In the absence of medication, the patient's condition and elevated ALT level improved within a month. Anti-HBe became detectable, and HBeAg disappeared 2 mo after onset of the symptoms. HBsAg became undetectable at 5 mo, but the patient still tested positive for HBV-DNA, a status that persisted for at least 26 mo following his presentation at our hospital (Figure 1). We are now preparing to administer anti-viral medication.

For further analysis of the HBV infecting this patient, HBV-DNA was extracted from the acute-phase serum using a QIAamp DNA Blood Mini kit (QIAGEN, Valencia, CA). The entire HBV genome sequence was determined after polymerase chain reaction (PCR) amplification using the following primers [the number of nucleotides (nt) added to the primers were deduced from the prototype HBV/C clone, with accession no. AB246344]. For the amplification of half of the HBV genome, the outer primers were 5'-ATTCCACCAAGCTCTGCTAG-ATCCCAGAGT-3' (nt 10-39) and 5'-GGTGCTGGT-GAACAGACCAATTTATGCCTA-3' (nt 1813-1784), and the inner primers were 5'-CCTATATTTTCCTGCT-GGTGGCTCCAGTTC-3' (nt 46-75) and 5'-TAGCCTA-ATCTCCTCCC CCAACTCCTCCCA-3' (nt 1760-1731). For the other half of the HBV genome, the outer primers were 5'- ACGTCGCATGGAGACCACCGTGAAC-GCCCA-3' (nt 1601-1630) and 5'-AAGTCCACCAC-GAGTCTAGACTCTGTGGTA-3' (nt 266-237), and the inner primers were 5'-CCAGGTCTTGCCCAAGGTCT-TACATAAGAG-3' (nt 1631-1660) and 5'-CCCGCCT-GTAACACGAGCAGGGGTCCTAGG-3' (nt 207-178). The PCR was performed in a thermal cycler for 30 cycles

Table 1 Laboratory findings at first visit to our hospital

Hematology		Blood chemistry		Viral markers		Immunology		Coagulation	
WBC	7400/μL	TP	7.4 g/dL	Anti-HA IgM	(-)	IgA	183 mg/dL	PT%	95%
Neutrophil	72.0%	Albumin	4.5 g/dL	Anti-HCV	(-)	IgG	1168 mg/dL	APTT	36.4 s
Eosinophil	1.0%	T-Bil	11.1 mg/dL	HBsAg	(+) 197333	IgM	220 mg/dL		
Basophil	0.0%	D-Bil	8.0 mg/dL	Anti-HBc IgM	(+) 25.5 C.O.I	ANA	× 40, homogeneous		
Monocyte	10.0%	AST	1942 IU/L	HBeAg	(+) 253 C.O.I				
Lymphocyte	17.0%	ALT	2963 IU/L	Anti-HBe	(-) 0.0 %				
RBC	457/μL	ALP	612 IU/L	HBV-DNA	7.7 log copies/mL				
Hemoglobin	16.0 g/dL	γGTP	756 IU/L	Anti-HIV	(-)				
Hematocrit	46.4%	LDH	739 IU/L	RPR	(-)				
Platelet	36.6 × 10⁴/μL	BUN	8.2 mg/dL	TPHA	(+)				
		Creatinine	0.64 mg/dL	Anti-CMV IgG	(+)				
		T-Chol	225 mg/dL	Anti-CMV IgM	(-)				
				Anti-EBV EBNA	(+)				
				Anti-EBV EA IgG	(-)				
				Anti-EBV VCA IgG	(+)				
				Anti-EBV VCA IgM	(-)				

WBC: White blood cells; RBC: Red blood cells; ANA: Antinuclear antibody; TP: Total protein; T-Bil: Total bilirubin; D-Bil: Direct bilirubin; AST: Aspartate aminotransferase; ALT: Alanine aminotransferase; ALP: Alkaline phosphatase; γGTP: γ-glutamyltranspeptidase; LDH: Lactase dehydrogenase; BUN: Blood urea nitrogen; T-Chol: Total cholesterol; PT: Prothrombin activity; APTT: Activated partial thromboplastin time; C.O.I: Cutoff index; HA: Hepatitis A; HCV: Hepatitis C virus; HBsAg: Hepatitis B surface antigen; HBc: Hepatitis B core; HBeAg: Hepatitis B e-antigen; HBV: Hepatitis B virus; HIV: Human immuno-deficiency virus; RPR: Rapid plasma regain; TPHA: Treponema pallidum hemagglutination assay; CMV: Cytomegalovirus; EBV: Epstein-Barr virus; EBNA: Epstein-Barr virus nuclear antigen; EA: Early antigen; VCA: Viral capsid antigen.
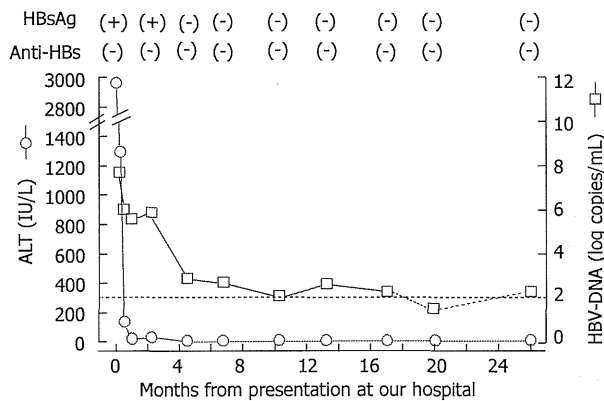

Figure 1 Clinical course of the patient infected with the genotype H strain. The dotted line indicates the detection limit of HBV-DNA (2.1 log copy/mL); the titer of the HBV-DNA was below the lower limit at 18 mo. HBsAg: Hepatitis B surface antigen; Anti-HBs: Antibody to hepatitis B surface antigen; ALT: Alanine aminotransferase; HBV: Hepatitis B virus.

(94 ℃, 30 s; 60 ℃, 30 s; 72 ℃, 30 s) with TAKARA LA Taq® DNA polymerase (TAKARA, Shiga, Japan). The amplified fragments were sequenced directly with an automated DNA sequencer (3500 Genetic Analyzer, Applied Biosystems, Foster City, CA, United States).

The genome of the infecting HBV (designated as B-MHJ9014) was 3215 bases in size. A phylogenetic analysis was performed with this strain and several database reference strains. B-MHJ9014 sorted with the genotype-H branch of the tree and clustered with the genotype-H strains previously isolated from Japanese patients (Figure 2). The substitutions at nt 1762 and nt 1764 (the basal core promoter region) and at nt 1896 (the precore region) were not observed. The length of the deduced amino acid sequences of the S, X, Core, and P proteins were identical to those encoded by other genotype H strains in

the databases. The α determinant region of the S protein of B-MHJ9014 harbored an amino acid polymorphism (phenylalanine to leucine) at residue 134. The predicted B-MHJ9014 reverse transcriptase did not include any of the amino acid substitutions known to be associated with nucleotide analog resistance. To assess the complexity of the infecting virus, S region sequences from 51 clones in acute phase serum were determined. The detected sequences were genotype H and were closely related to the consensus sequence determine by direct sequencing with 1-3 amino acids polymorphisms (data not shown).

To assess the presence of human genome SNPs in the HLA-DP locus that are associated with persistent infection by HBV[14,15], a blood specimen was obtained from the patient (who had previously provided informed consent). Genomic DNA was extracted from buffy coat samples with the QIAamp DNA Mini kit (QIAGEN); DNA for SNPs rs3077 and rs9277535 were amplified with the appropriate primers and TAKARA LA Taq® DNA polymerase and were sequenced directly. The patient was homozygous (G/G) at both of these SNPs; these alleles are considered to be risk alleles for persistent infection.

DISCUSSION

HBV genotype H was first reported in 2002[5]. Infections by this genotype have been found mainly in Nicaragua, Mexico, and California; this genotype is considered to be rare in Asia, particularly in Japan[5,16-18]. However, since the first recognition of genotype H in Japan in 2005, eight strains have been isolated from Japanese patients (Table 2)[18-25]. All reported genotype H strains were isolated from male patients aged 35 to 65 years old, and the major route of infection was sexual transmission (5/8, 62.5%). Four cases (50%) represent transmissions that
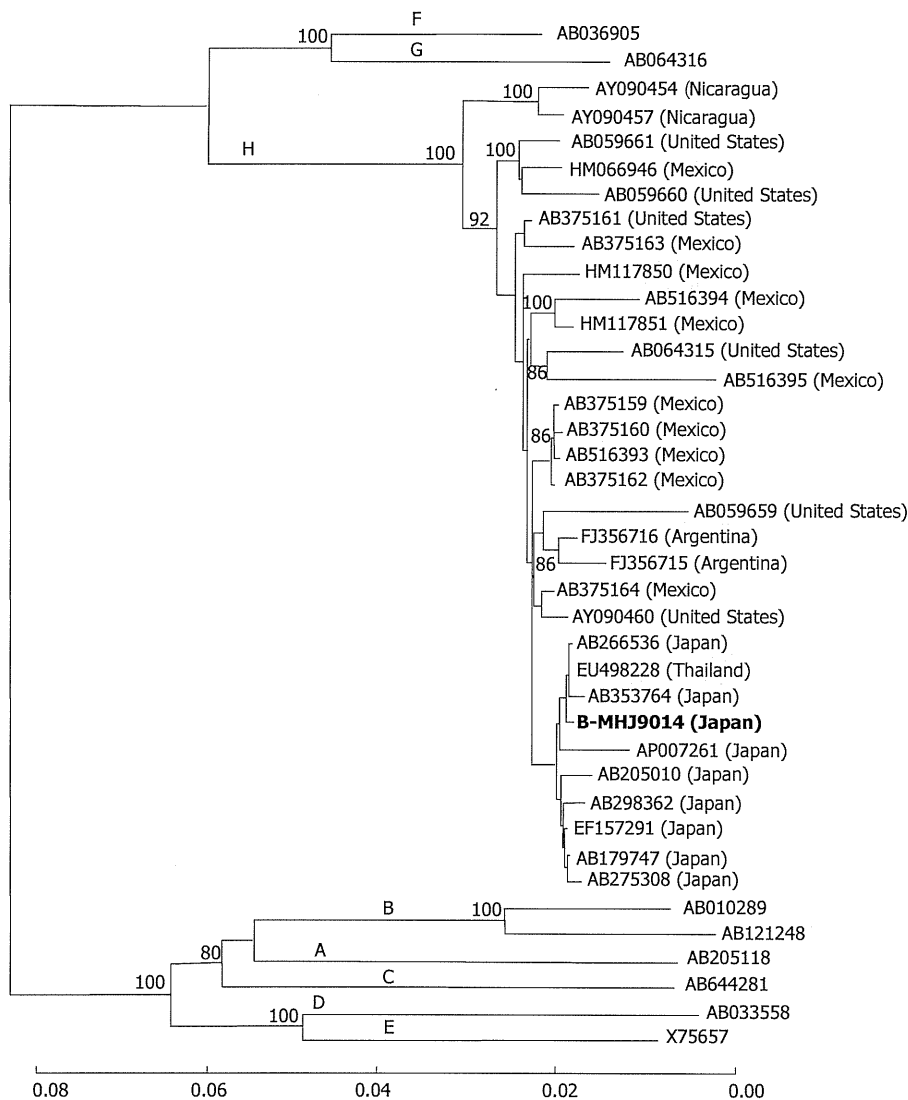
Figure 2 A phylogenetic trees constructed using the neighbor-joining method with the full hepatitis B virus genome sequence of the isolated and reference strains. The strain isolated in this case (B-MHJ9014) is shown in bold. The horizontal bar indicates the number of nucleotide substitutions per site. The reference sequences are shown with the DDBJ/EMBL/GenBank accession numbers. The HBV genotypes are indicated on each branch. The bootstrap values (> 80%) are indicated at the nodes as a percentage of the data obtained from 1000 resamplings. HBV: Hepatitis B virus.

Table 2 Genotype H strains reported in Japan

No.	Patient		Hypothesized source of infection		HIV infection[1]	Clinical feature	Accession number (Ref.)
	Age	Gender	Route	Place			
1	52	Male	Unknown	Japan	NA	Unknown blood donor	AB179747, [18]
2	61	Male	Sexual contact (heterosexual)	Thailand	NA	Chronic	AB205010, [19]
3	46	Male	Sexual contact (bisexual)	South America	(+)	Chronic	AP007261, [20]
4	38	Male	Sexual contact (homosexual)	Unknown	NA	Chronic	AB298362, [21]
5	65	Male	Unknown	Japan	NA	Acute	EF157291, [22]
6	35	Male	Unknown	Japan	NA	Acute	AB266536, [23]
7	60	Male	Sexual contact (homosexual)	Japan	(-)	Acute	AB275308, [24]
8	60	Male	Sexual contact (heterosexual)	Unknown	(+)	Chronic	AB353764, [25]
9	47	Male	Unknown	Japan	(-)	Acute to chronic	AB846650, this paper

[1]NA: Not available; HIV: Human immunodeficiency virus.

occurred in Japan. Co-infection with HIV was not common (2/8, 25%). These characteristics were similar to the case described here. All isolated strains from Japanese patients clustered together as a branch on the phyloge-

netic tree; therefore, it is possible that a specific strain of genotype H has emerged and spread in Japan. Presumably, the infrequent use of a reliable and convenient detection kit for genotype H infection has hampered the

correct diagnosis of genotype H infection; some cases may be misdiagnosed and considered to be infections by other genotypes. In fact, in the current case, our HBV isolate was originally identified as genotype C by the commercial kit that is covered by insurance in Japan. This kit was developed before the discovery of genotype H; thus, such a misidentification is a potential risk, as noted in the kit's instruction manual. The clinical features of genotype H infection remain obscure. There is a growing need for an accumulation of genotype H infection cases. To this end, the use of a reliable HBV genotyping kit that can correctly distinguish all genotypes is essential for routine clinical practice.

In Japan, most cases of acute hepatitis B are self-limiting, but some cases have been reported to have progressed to persistent infections[9,26-29]. Among the reported cases of genotype H infection, 4 strains were isolated from chronic hepatitis patients; in all cases, the infection was ascribed to sexual contact (Table 2)[19-21,25]. In our case, the HBV-DNA persisted for at least 26 mo. To our knowledge, this report represents the only case of genotype H infection in which chronic hepatitis was observed following acute infection. HBsAg was no longer detected at 4 mo from onset by HISCL-2000i. This disappearance was also confirmed by ARCHITECT® HBsAg (CMIA, Abbott Japan, Tokyo, Japan). In the S protein analysis, we found an amino acid polymorphism in the α determinant region. This polymorphism may affect the sensitivity for detecting HBsAg. HIV infection, a well-known risk factor for prolonged HBV infection[30], was not detected in our patient. Recently, the risk factors for HBV persistent infection have been reported in an analysis of a cohort that excluded patients co-infected with HIV[29]. In that report, infection with genotype A, elevated peak levels of HBV-DNA, and attenuated peak levels of ALT were suggested as risk factors for chronic infection. In the case described here, the peak level of HBV-DNA was 7.7 log copy/mL, which was consistent with increased risk for chronic infection. However, our patient exhibited a peak level of ALT of 2963 IU/L, which is a value that would classify this individual in the self-limiting group. Therefore, the clinical features of this case did not completely fit the risk factors associated with the establishment of chronic infection in the previous analysis[29]. Another reported risk factor for chronic HBV infection is the presence of certain SNP alleles. Specifically, selected SNPs around the HLA-DP locus have been reported to be associated with chronic hepatitis B in Asians[14,15]. With the informed consent of our patient, we determined the sequences for these SNPs (rs3077 and rs9277535) and found that this patient harbored risk alleles at both polymorphisms. This factor may have contributed to the establishment of chronic infection in this case.

In conclusion, we report a case of acute hepatitis B caused by a genotype H strain of HBV. This patient exhibited persistent infection. Our finding suggests that the infection of HBV genotype H can be a risk factor for persistent infection. We believe that it is necessary to use kits that are capable of accurate genotyping to permit an ac-

cumulation of cases and to investigate the clinical features of genotype H infection in routine clinical practice.

COMMENTS

Case characteristics
The main symptoms were nausea, loss of appetite, and a feeling of fullness in the abdomen.

Clinical diagnosis
The patient was a case of acute hepatitis B caused by a genotype H strain with persistent infection.

Differential diagnosis
The hepatitis B virus (HBV) genotype was considered to be important to predict the outcome and clinical features.

Laboratory diagnosis
To diagnose this patient, the detection of HBV markers and the complete determination of the HBV genotype were essential.

Treatment
The anti-viral treatment was not administered because we expected this case was self-limiting. Authors are now preparing medication.

Experiences and lessons
The infection of HBV genotype H can be a risk factor for persistent infection and the complete determination of HBV genotype is important.

Peer review
To conclude the association between HBV genotype H and chronic infection, the accumulation of cases of genotype H infection is essential.

REFERENCES

1   **World Health Organization**. Hepatitis B Fact Sheet. Accessed August 2013. Available from: URL: http://www.whoint/mediacentre/factsheets/fs204/en/indexhtml
2   **Okamoto H**, Tsuda F, Sakugawa H, Sastrosoewignjo RI, Imai M, Miyakawa Y, Mayumi M. Typing hepatitis B virus by homology in nucleotide sequence: comparison of surface antigen subtypes. *J Gen Virol* 1988; **69** (Pt 10): 2575-2583 [PMID: 3171552 DOI: 10.1099/0022-1317-69-10-2575]
3   **Norder H**, Couroucé AM, Magnius LO. Complete genomes, phylogenetic relatedness, and structural proteins of six strains of the hepatitis B virus, four of which represent two new genotypes. *Virology* 1994; **198**: 489-503 [PMID: 8291231 DOI: 10.1006/viro.1994.1060]
4   **Stuyver L**, De Gendt S, Van Geyt C, Zoulim F, Fried M, Schinazi RF, Rossau R. A new genotype of hepatitis B virus: complete genome and phylogenetic relatedness. *J Gen Virol* 2000; **81**: 67-74 [PMID: 10640543]
5   **Arauz-Ruiz P**, Norder H, Robertson BH, Magnius LO. Genotype H: a new Amerindian genotype of hepatitis B virus revealed in Central America. *J Gen Virol* 2002; **2002**: 2059-2073
6   **Kurbanov F**, Tanaka Y, Mizokami M. Geographical and genetic diversity of the human hepatitis B virus. *Hepatol Res* 2010; **40**: 14-30 [PMID: 20156297 DOI: 10.1111/j.1872-034X.2009.00601.x]
7   **Kobayashi M**, Arase Y, Ikeda K, Tsubota A, Suzuki Y, Saitoh S, Kobayashi M, Suzuki F, Akuta N, Someya T, Matsuda M, Sato J, Kumada H. Clinical characteristics of patients infected with hepatitis B virus genotypes A, B, and C. *J Gastroenterol* 2002; **37**: 35-39 [PMID: 11824798]
8   **Tamada Y**, Yatsuhashi H, Masaki N, Nakamuta M, Mita E, Komatsu T, Watanabe Y, Muro T, Shimada M, Hijioka T, Satoh T, Mano Y, Komeda T, Takahashi M, Kohno H, Ota H, Hayashi S, Miyakawa Y, Abiru S, Ishibashi H. Hepatitis B virus strains of subgenotype A2 with an identical sequence spreading rapidly from the capital region to all over Japan in patients with acute hepatitis B. *Gut* 2012; **61**: 765-773 [PMID: 22068163 DOI: 10.1136/gutjnl-2011-300832]
9   **Yotsuyanagi H**, Ito K, Yamada N, Takahashi H, Okuse C, Yasuda K, Suzuki M, Moriya K, Mizokami M, Miyakawa Y,